Available online at www.sciencedirect.com
ScienceDirect
Journal of Energy Chemistry 22(2013)72–77
JOURNAL OF ENERGY CHEMISTRY
www.elsevier.com/journals/journal-of-energy-chemistry/2095-4956
www.elsevier.com/locate/jngc

A quantum-chemical study on the discharge reaction mechanism of lithium-sulfur batteries

Lijiang Wang, Tianran Zhang, Siqi Yang, Fangyi Cheng, Jing Liang, Jun Chen*

Key Laboratory of Advanced Energy Materials Chemistry (Ministry of Education), College of Chemistry, Nankai University, Tianjin 300071, China

[Manuscript received November 20, 2012; revised December 10, 2012]

Abstract

Lithium-sulfur batteries have attracted a great interest in electrochemical energy conversion and storage, but their discharge mechanism remains not well understood up to now. Here, we report density functional theory (DFT) calculation study of the discharge mechanism for lithium-sulfur batteries which are based on the structure of S_8 and Li_2S_x ($1\leq x\leq 8$) clusters. The results show that for Li_2S_x ($1\leq x\leq 8$) clusters, the most stable geometry is chainlike when $x = 1$ and 6, while the minimal-energy structure is found to be cyclic when $x = 2$–5, 7, 8. The stability of Li_2S_x ($1\leq x\leq 8$) clusters increases with the decreasing x value, indicating a favorable thermodynamic tendency of transition from S_8 to Li_2S. A three-step reaction route has been proposed during the discharge process, that is, $S_8\rightarrow Li_2S_4$ at about 2.30 V, $Li_2S_4\rightarrow Li_2S_2$ at around 2.22 V, and $Li_2S_2\rightarrow Li_2S$ at 2.18 V. Furthermore, the effect of the electrolyte on the potential platform has been also investigated. The discharge potential is found to increase with the decrease of dielectric constant of the electrolyte. The computational results could provide insights into further understanding the discharge mechanism of lithium-sulfur batteries.

Key words

lithium-sulfur battery; density functional theory; discharge mechanism; lithium polysulfide; discharge potential

1. Introduction

Lithium-sulfur (Li–S) batteries have attracted increasing attention due to their high theoretical specific capacity of 1675 $mAh\cdot g^{-1}$ and high theoretical energy density of 2600 $Wh\cdot kg^{-1}$ [1], which dramatically outperform those of commercial lithium-ion batteries [2]. In addition, sulfur has the advantages of high natural abundance, light equivalent weight, low cost and mild environmental impact [3]. In a typical discharge process of Li-S batteries, metallic lithium anode reacts with elemental sulfur (S_8) cathode to form lithium polysulfide (Li_2S_x), with the final product being lithium sulfide (Li_2S) [3−5]. However, the discharge process of sulfur electrode remains unclear though several mechanisms have been proposed [4,6−10].

In 1980s, the redox processes of Li_2S_x ($6\leq x\leq 12$) were electrochemically investigated on a glassy carbon electrode in tetrahydrofuran (THF) [6]. Three cathodic peaks were detected in a diffusion-controlled reaction and were attributed to the reduction of element sulfur (S_8) to S_6^{2-}, S_6^{2-} to S_5^{2-} and S_5^{2-} to S_2^{2-} and/or S^{2-}, respectively. Recent studies have indicated that the cathode redox reactions involve $S_8\rightarrow Li_2S_8\rightarrow Li_2S_6\rightarrow Li_2S_4\rightarrow Li_2S_2\rightarrow Li_2S$ [7–9] or $S_8\rightarrow Li_2S_8\rightarrow Li_2S_4\rightarrow Li_2S_2\rightarrow Li_2S$ [4]. Lately, a new mechanism was reported for sulfur reduction, which consists of three steps based on the dissolution of active materials during cycling [10]. At the preliminary step, S_8^{2-} and S_6^{2-} are generated (2.4−2.2 V vs Li^+/Li). Then, S_4^{2-} is formed during the second stage (2.15−2.1 V vs Li^+/Li). Finally, S_3^{2-}, S_2^{2-} and S^{2-} are produced in the end of the reduction process (2.1−1.9 V vs Li^+/Li). Thus, the type of intermediate species involved in the cathode reactions is still in debate. In addition, the reported two-plateau reduction process in literatures [3,5,11−13] is not consistent with the three-plateau reduction process in other reports [1,2,14]. Therefore, to develop advanced Li-S batteries, a better understanding of the discharge mechanism of sulfur electrode is of great interest and importance.

However, it is a challenge to experimentally investigate the discharge mechanism of Li–S batteries because of the

* Corresponding author. Tel: +86-22-23506808; Fax: +86-22-23509571; E-mail: chenabc@nankai.edu.cn
This work was supported by the Programs of National 973 (2011CB935900), NSFC (21076108) and 111 Project (B12015).

complex intermediate species involved in the sulfur electrode. In comparison, density functional theory (DFT) calculation has been proved as a useful tool to study the reaction mechanism of a variety of electrode materials such as Li_xFePO_4, Li_xTiS_2, Si and Li_xTiP_4 [15−18]. To the best of our knowledge, there has been few DFT study on the discharge mechanism of Li-S batteries. It is thus that we report a quantum-chemical investigation on the reaction mechanism of the sulfur electrode of Li-S batteries. The structures of Li_2S_x ($1\leq x\leq 8$) clusters are identified and the possible discharge mechanism is proposed on the basis of DFT calculation. Furthermore, theoretical modeling has also been performed on the effect of the electrolyte. The results could help further understanding of the discharge processes of sulfur electrode of rechargeable Li-S batteries.

2. Computational details and models

2.1. Computational details

Standard DFT and electronic-structure calculations were carried out using Gaussian 03 software package [19]. The geometries were fully optimized for each cluster using Becky's three-parameter exchange function combined with Lee-Yang-Parr correlation functional (B3LYP) [20,21]. We initially optimized these structures at B3LYP/6-31G (d) theoretical level. The obtained geometries were refined with B3LYP/6-311G (3df) method. Functional and basis set effects were considered. Vibration frequency calculations were performed to verify the true minima and to derive corrections for zero-point energy. The solvent effect to the electrode potential was evaluated by polarizable continuum model (PCM) [22]. The average stabilization energy [23] and average Gibbs free energy difference were presented to interpret the relative stability and reaction trend of Li_2S_x ($1\leq x\leq 8$). The possible potential plateaus were speculated by calculating the standard Gibbs free energy of reaction [24].

2.2. Models

Sulfur is a typical molecular crystal at room temperature. The orthorhombic α-sulfur is the most stable form at standard temperature and pressure, consisting of many cycloocta-S (S_8) molecules. Hence, we chose S_8 cluster as basic model for the calculations. Cycloocta-S has the crown shape and D_{4d} symmetry [25]. During the discharge process of lithium-sulfur batteries, S–S covalent bonds of Cycloocta-S are broken to form lithium polysulfides Li_2S_x ($2\leq x\leq 8$) which are further reduced into Li_2S through multistage reactions. However, the exact number of stable lithium polysulfide Li_2S_x ($1\leq x\leq 8$) during the discharge process of lithium-sulfur batteries has not yet been proved beyond doubt by now. Hence all possible geometries of S_8 and Li_2S_x ($1\leq x\leq 8$) were fully optimized at B3LYP/6-311G (3df) theoretical level with zero-point vibrational energies (ZPVEs).

3. Results and discussion

3.1. Structures of S_8 and Li_2S_x ($1\leq x\leq 8$) clusters

3.1.1. S_8

Figure 1 shows the calculated most stable structure of S_8 with values of the inter-atomic distances and bond angles, which can be assigned to D_{4d} symmetric. The optimized S–S bond length in S_8 is 2.072 Å and the S–S–S angle is 108.9°. The optimized S–S bond lengths, S–S–S bond angles and S–S–S–S dihedral angles in S_8 at B3LYP/6-311G(3df) level only have a gap of 0.009 Å, 0.2° and 0° in comparison with the experimental values, respectively. It proved that B3LYP is a good choice of functional for geometry optimization.

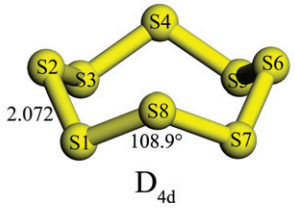

Figure 1. Optimized geometries and major structural parameters of S_8 at B3LYP/6-311G (3df) level and the selected bond lengths (Å) and angles (°)

To obtain more correct calculation results, the effects of basis set on the geometry parameters of S_8 are discussed and listed in Table 1. The results indicate that as basis set increases, the goodness of fit increases firstly and drops slightly afterward in the experimental values, and it can clearly be seen that the geometry parameters of S_8 at B3LYP/6-311G (3df) level are better than those of B3LYP/6-311+G (3df) level.

Table 1. Calculated and experimental structure parameters of S_8

Geometry parameters	B3LYP/6-31G (d)	B3LYP/6-311G (d)	B3LYP/6-311G (3df)	B3LYP/6-31+G (3df)	Experimental [25]
Symmetry	D_{4d}	D_{4d}	D_{4d}	D_{4d}	D_{4d}
S–S (Å)	2.100	2.110	2.072	2.073	2.060±0.003
S–S–S (°)	109.163	109.070	108.900	108.915	108.0±0.7
S–S–S–S (°)	97.352	97.467	97.675	97.657	98.3±2.1

To further confirm the accuracy of the method, infrared and Raman frequencies of S_8 at B3LYP/6-311G (3df) level have been calculated and the results compared with experimental values of α-sulfur at 30 K are summarized in Table 2. It is clearly seen that the spectral parameters of S_8 based on DFT calculations well agree with the experimental data.

Table 2. Calculated and observed infrared and Raman frequencies of sulfur (cm^{-1}) at 30 K

Calculated (S_8)		Experimental (α-sulfur) [25]	
(11 fundamentals)	designation	(11 fundamentals)	designation[a]
ν_1 = 469.59		ν_1 = 475	
ν_2 = 213.97	a_1 R	ν_2 = 218	a_1 R
ν_3 = 375.63	b_1 I	ν_3 = 411	b_1 I
ν_4 = 241.40	b_2 Ir	ν_4 = 243	b_2 Ir
ν_5 = 460.85		ν_5 = 471	
ν_6 = 190.25	e_1 Ir	ν_6 = 191	e_1 Ir
ν_7 = 454.47		ν_7 = 475	
ν_8 = 144.38		ν_8 = 152	
ν_9 = 73.42	e_2 R	ν_9 = 86	e_2 R
ν_{10} = 403.09		ν_{10} = 437	
ν_{11} = 248.45	e_3 R	ν_{11} = 248	e_3 R

[a] R = Raman active, I = inactive, and Ir = infrared active

3.1.2. Li_2S_x ($1 \le x \le 8$) clusters

Figure 2 shows the optimized geometry structures and structural parameters of Li_2S_x ($1 \le x \le 8$) clusters. The most stable structure of Li_2S is a chainlike form with C_{2v} symmetry. The ground state structure of Li_2S_2 is a tridimensional monocyclic ring with C_s symmetry. For Li_2S_3, it has the tetrahedral shape and C_1 symmetry. Beyond that, Li_2S_3 adds two S–S bonds. Both Li_2S_4 and Li_2S_5 have similar three-ring structures and C_1 symmetry. For $x = 6$, the lowest-energy geometry is that terminated by sulfur atom on both sides of the structure. It is an open-chain structure with C_1 symmetry. For Li_2S_7 and Li_2S_8, the lowest-energy structure is eight-member and nine-member ring with a branching chain, respectively. Both of them have the same C_1 symmetry. Above all, for Li_2S_x ($1 \le x \le 8$) clusters, when $x = 1$ or 6, the most stable geometry is chainlike, while x stands for other values, the minimal-energy structure is found to be cyclic. Moreover, we found that the distance for Li–S bond (2.073 Å) in Li_2S is shortened by about 10% compared with that of the same bond in Li_2S_8 (2.354, 2.348, 2.340 Å), implying that the interaction of Li–S strengthens with the decrease of x value in Li_2S_x clusters. Whereas, S–S distance in Li_2S_4 is only 0.004 Å longer than that of the same bond in S_8. It shows that there is no obvious change for the interaction of S–S in Li_2S_x clusters.

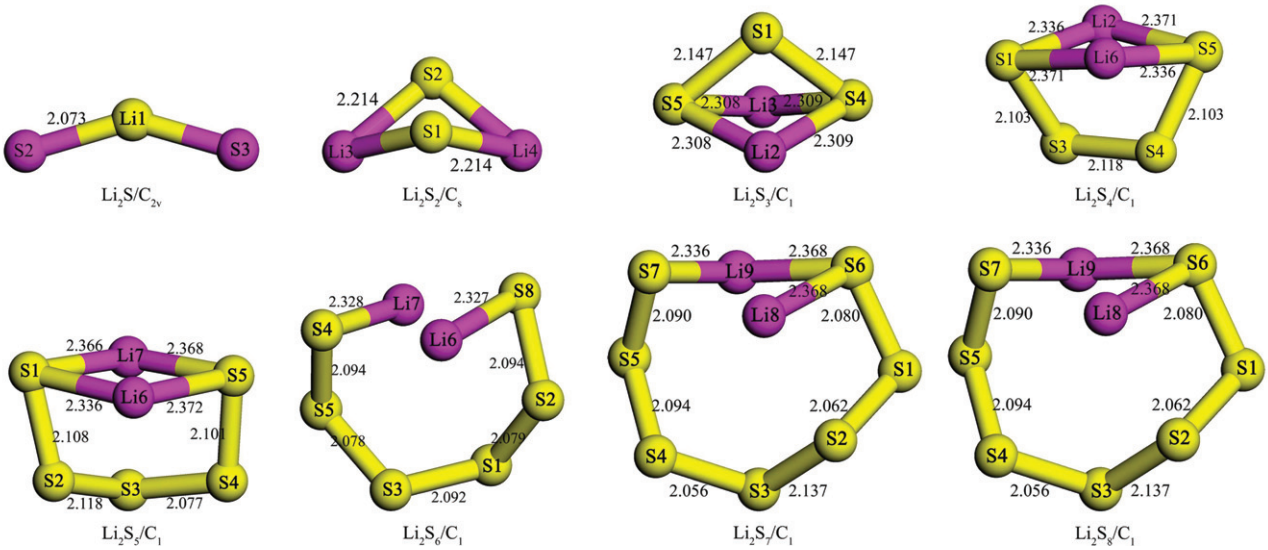

Figure 2. Optimized geometries, structural parameters of Li_2S_x ($1 \le x \le 8$) clusters at B3LYP/6-311G (3df) level and the selected bond lengths (Å)

3.2. Discharge mechanisms

3.2.1. ΔE_{ave} and ΔG_{ave} of Li_2S_x ($1 \le x \le 8$) clusters

For the sake of comparison, the average stabilization energy (ΔE_{ave}) [23] is presented to interpret the relative stability of Li_2S_x and S_8 according to the reaction

$$x/8S_8 + 2Li = Li_2S_x$$

and is calculated as

$$\Delta E_{ave} = [H_f^o(Li_2S_x) - 2H_f^o(Li)]/x - H_f^o(S_8)/8$$

It is clear that the more negative value of ΔE_{ave}, the greater the stability is. The results shown in Figure 3 demonstrate that all Li_2S_x (x = 1–8) clusters are relatively more stable than S_8. For Li_2S_x (x = 1–8) clusters, the stability sequence is $Li_2S > Li_2S_2 > Li_2S_3 > Li_2S_4 > Li_2S_5 > Li_2S_6 > Li_2S_7 > Li_2S_8 > S_8$.

At the same time, we put forward an average Gibbs free energy difference (ΔG_{ave}) to explain the relative reaction trend of Li_2S_x and S_8 according to the reaction

$$x/8S_8 + 2Li = Li_2S_x$$

and is calculated as

$$\Delta G_{ave} = [G_f^o(Li_2S_x) - 2G_f^o(Li)]/x - G_f^o(S_8)/8$$

It is obviously that the more negative the value of ΔG_{ave}, the greater the reaction trends. Figure 3 shows a clear trend of ΔG_{ave} decrease as x value in Li_2S_x (x = 1–8) lessens. For example, x = 8, ΔG_{ave} = −65.670 kJ·mol^{-1}; x = 4, ΔG_{ave} decreases from −65.670 to −129.372 kJ·mol^{-1}; x = 1, ΔG_{ave} substantially decreases to −336.195 kJ·mol^{-1}. Our interpretation from Figure 3 is that during the discharge process S_8 has an obvious trend of turning into Li_2S.

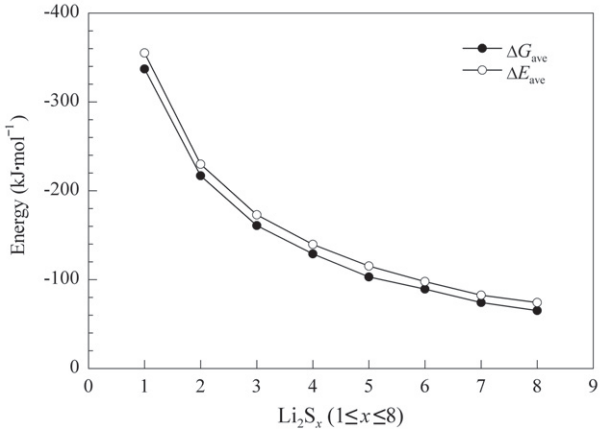

Figure 3. Average stabilization energies (ΔE_{ave}) of Li_2S_x ($1 \le x \le 8$) clusters and average Gibbs free energy differences (ΔG_{ave}) of sulfur between Li_2S_x ($1 \le x \le 8$) and S_8 clusters at B3LYP/6-311G (3df) level

3.2.2. Discharge mechanisms

Sulfur reduction is a multiple-step electro-chemical process that can include the sequential formation of different intermediate products [6,9]. Elemental sulfur (S_8) reacts with metallic lithium to produce lithium polysulfide with a general expression of Li_2S_x ($1 \le x \le 8$). At the end of the discharge, the final product is lithium sulfide (Li_2S). For this reason, we have researched the discharge reaction mechanism of Li–S batteries on the basis of every unit of S_8 and the sequential intermediates Li_2S_x react with two units of lithium metal every step. Table 3 summarizes the standard Gibbs free energies ($\Delta_r G^o$) and cell potentials (E^o) of possible reactions. As a preliminary step, S_8 reacts with two lithium atoms to produce Li_2S_8. For the next step, there are four possibilities corresponding to Li_2S_4, Li_2S_5+Li_2S_3, Li_2S_6+Li_2S_2 or Li_2S_7+Li_2S after a Li_2S_8 accepts two lithium atoms. Thus, we judge the reaction trend and potential plateau corresponding to reaction by the following formula:

$$E^o = -\Delta_r G^o / ZF$$

where, F is Faraday constant, E^o is the battery voltage corresponding to reaction, $\Delta_r G^o$ is the standard Gibbs free energy of reaction at 298.15 K. $\Delta_r G^o$ and E^o for the reaction are listed in Table 3. The corresponding $\Delta_r G^o$ of Reactions (2)−(5) are −509.610, −484.142, −441.872, −337.902 kJ·mol^{-1}, respectively. The $\Delta_r G^o$ of Reaction (2) has the energy 25.47, 67.74, 171.71 kJ·mol^{-1} lower than those of the Reactions (3)–(5), respectively. It is indicated that the tendency of reaction is predicted as Li_2S_4>Li_2S_5+Li_2S_3>Li_2S_6+Li_2S_2>Li_2S_7+Li_2S from the Gibbs free energy analysis. Hence, Li_2S_4 is the foremost intermediate. At the same time, there may be a small amount of Li_2S_5 and Li_2S_3 in the intermediates. In the third step, the main reaction that Li_2S_4 accepted lithium atoms to turn into Li_2S_2 corresponds to Reaction (6). However, Li_2S_5 will turn into Li_2S_3 and Li_2S_2 before Li_2S_4 transforms into Li_2S_2 if there is a small quantity of Li_2S_5 and Li_2S_3 in the above step, with the corresponding average potential of 2.03 V. At last, a Li_2S_2 molecule reacts with two lithium atoms to produce two Li_2S. Li_2S_3 will also transform into Li_2S_2 and Li_2S before Li_2S_2 reacts with lithium atoms if there is a small quantity of Li_2S_3 and Li_2S_2 in the previous step. Therefore, it can be seen that the discharge mechanism of Li–S batteries is a very complex process. As a conclusion, the main reactions for sulfur reduction can be summarized as follows: $S_8 \rightarrow Li_2S_8 \rightarrow (Li_2S_4)_2 \rightarrow (Li_2S_2)_4 \rightarrow (Li_2S)_8$.

Table 3. $\Delta_r G^o$ and E^o of possible chemical reactions

Serial number	Reactions	$\Delta_r G^o$/kJ·mol^{-1}	E^o/V
(1)	S_8+2Li → Li_2S_8	−525.363	2.72
(2)	Li_2S_8+2Li → Li_2S_4	−509.610	2.64
(3)	Li_2S_8+2Li → Li_2S_3+Li_2S_5	−484.142	2.51
(4)	Li_2S_8+2Li → Li_2S_6+Li_2S_2	−441.872	2.29
(5)	Li_2S_8+2Li → Li_2S_7+Li_2S	−337.902	1.75
(6)	Li_2S_4+2Li → 2Li_2S_2	−386.829	1.80
(7)	Li_2S_4+2Li → Li_2S_3+Li_2S	−303.508	1.57
(8)	Li_2S_5+2Li → Li_2S_3+Li_2S_2	−392.250	2.03
(9)	Li_2S_5+2Li → Li_2S_4+Li_2S	−328.975	1.70
(10)	Li_2S_3+2Li → Li_2S_2+Li_2S	−283.554	1.46
(11)	Li_2S_2+2Li → Li_2S	−240.233	1.24
(12)	S_8+2Li → Li_2S_8	−410.891	2.13
(13)	Li_2S_8+2Li → $(Li_2S_4)_2$	−476.003	2.47
(14)	1/2 $(Li_2S_4)_2$+2Li → 1/2$(Li_2S_2)_4$	−428.744	2.22
(15)	1/4 $(Li_2S_2)_4$+2Li → 1/8 $(Li_2S)_8$	−420.080	2.18
(16)	S_8+4Li → $(Li_2S_4)_2$	−886.894	2.30

To obtain more accurate data, we had the average energies of $(Li_2S_4)_2$, $(Li_2S_2)_4$ and $(Li_2S)_8$ (Figure 4) instead of the energies of Li_2S_4, Li_2S_2 and Li_2S as a result of one S_8 formed in sequence two Li_2S_4, four Li_2S_2, eight Li_2S. Besides that, the Gibbs free energy of lithium was also corrected. Different starting geometries were used for Li_n with n ranging from 1 to 9, as shown in Figure 5. The corresponding absolute energy was primarily divided by the number of Li units in the cluster, and then scaled with Li as the reference energy. A normalized energy per Li atom unit was thus obtained. As we can see from Figure 5, when the cluster size goes up, the relative energy of the cluster becomes more negative and converges when $n \ge 8$. Therefore, the cluster of 9 Li formula units is used to reevaluate the main discharging potential plateau of Li–S batteries. The average Gibbs free energy (G_{ave}^o) of Li_2S_4, Li_2S_2 and Li_2S falls by −80.865, −118.410, −206.364 kJ·mol^{-1} after correction, respectively.

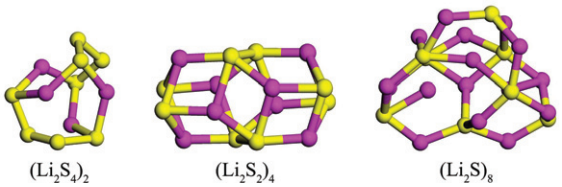

Figure 4. Optimized structures of $(Li_2S_4)_2$, $(Li_2S_2)_4$ and $(Li_2S)_8$ clusters at B3LYP/6-311G (3df) level

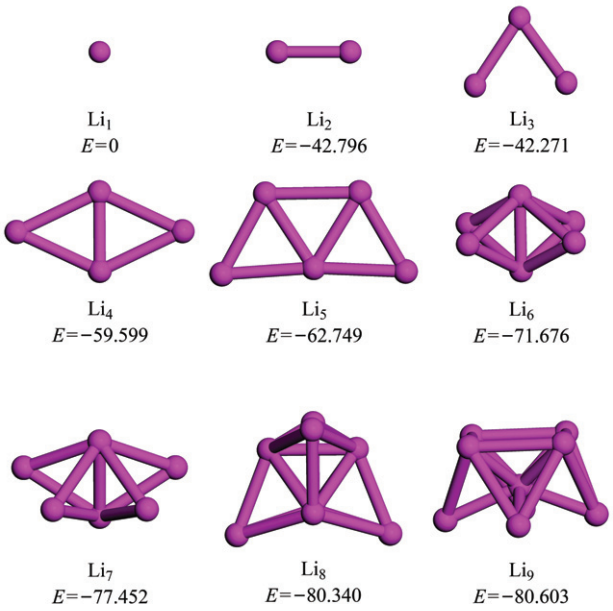

Figure 5. Optimized geometries and corresponding normalized energies (kJ·mol^{-1}) of Li_n clusters ($1 \le n \le 9$)

The standard battery potential (2.13 V) corresponding to Equation (12) in the first step reaction is lower than that of the second step reaction corresponding to Equation (13) after correction. Hence S_8 should directly react with four lithium atoms to form Li_2S_4. There is a potential plateau of 2.30 V corresponding to about 418.75 mAh·g^{-1} based on the theoretical calculation in this step. It agrees well with the peak at around 2.4 V in experiment [1,2,14]. The second voltage plateau at about 2.22 V should be assigned to the reduction of higher-order Li polysulfide Li_2S_4 to lower-order Li_2S_2, corresponding to the capacity of 418.75 mAh·g^{-1}. It is very close to the voltage plateau of about 2.1 V in experiment [1,2, 13,14]. The last potential platform at about 2.18 V, which is related to the reduction of Li_2S_2 to Li_2S, corresponds to the capacity of 837 mAh·g^{-1}. It is slightly lower than the second potential platform. This may be the main reason why we usually only observed two platforms. The main potential plateaus and the corresponding products were presented in Figure 6. It is worth noting that the electrical insulation of Li_2S_2 and Li_2S could still be one of the critical reasons of leading to low utilization of sulfur and low discharging rate. This problem could be alleviated by nanometer composite materials including metal or graphene with superior conductivity.

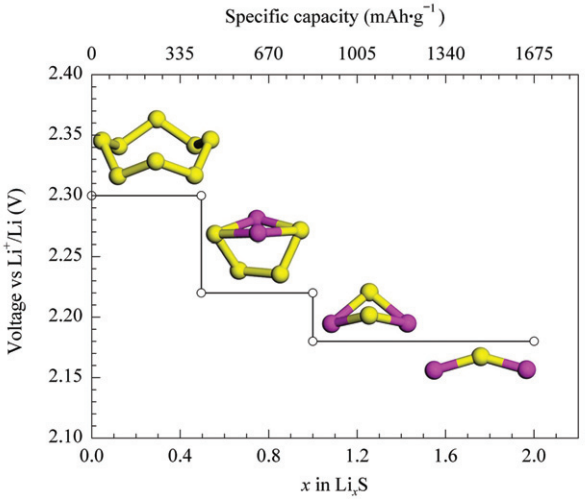

Figure 6. Structures and corresponding discharging potential plateaus of several kinds of lithium polysulfide

3.3. Effect of electrolyte

Besides concentration of lithium ion, discharge rate [5,13] and electrolyte additive [26,27], electrolyte [2,26,28,29] has an important effect on voltage plateau. Hence, We carried out calculations in nine kinds of electrolyte with B3LYP/6-311G(3df) level using PCM to evaluate the solvent effect on the electrode potential made up of lithium and lithium ions. The results are summarized in Table 4. We can conclude that the bigger the dielectric constant value (ε) of the electrolyte the greater the relative electrode potential ($\psi^{o}_{(Li^+/Li)}$) is. As a result, during the discharge process, the potential plateau of Li–S batteries will get lower. For example, the first potential platform for the three electrolytes is at about 2.15 V of a mixture of ethylene carbonate (ε = 95.3) and diethyl carbonate (ε = 3.15) (1 : 1, v/v) [29], 2.2 V of sulfolane (ε = 43.3), 2.4 V of 1,3-dioxolane (ε = 7.1) and 1,2-dimethoxyethane (ε = 7.2) (1 : 1, v/v) [26], respectively. Hence, electrolyte may be one of the reasons that make differences between the calculations and experimental results. In a word, it should be helpful to raise the potential of the plateau by means of selecting the electrolyte of low dielectric constant value, appropriate smaller concentration of lithium ion and suitable additive.

Table 4. The relative Gibbs free energies ($G^{o}_{Li^+}$) and electrode potential of lithium anode ($\psi^{o}_{(Li^+/Li)}$)

Electrolyte	ε^a	$G^{o}_{Li^+}$/kJ·mol^{-1}	$\psi^{o}_{(Li^+/Li)}$/V
C_6H_{12}	2.247	0	0
$C_6H_6CH_3$	2.379	−41.745	0.43
$(CH_3CH_2)_2O$	4.335	−149.128	1.55
C_6H_5Cl	5.621	−179.059	1.86
$C_6H_5NH_2$	6.89	−197.700	2.05
THF	7.58	−205.052	2.13
$(CH_3)_2CO$	20.7	−252.573	2.62
DMSO	46.7	−267.801	2.78
H_2O	78.39	−272.527	2.82

[a] Dielectric constant

4. Conclusions

We have employed DFT calculation to investigate the structures of Li_2S_x ($1 \leq x \leq 8$) cluster and the reaction mechanism of sulfur electrode during the discharge process. The results show that the most stable geometries of Li_2S and Li_2S_6 are chain-like, but the other minimal-energy structures are found to be cyclic in Li_2S_x ($1 \leq x \leq 8$) clusters. For S_8 and Li_2S_x, the stability sequence is $Li_2S > Li_2S_2 > Li_2S_3 > Li_2S_4 > Li_2S_5 > Li_2S_6 > Li_2S_7 > Li_2S_8 > S_8$, and S_8 has an obvious trend of turning into Li_2S. During the discharge process, the first potential plateau should be assigned to the reduction of elemental sulfur to higher-order Li_2S_4, and the second potential plateau should correspond to the reduction of higher-order Li_2S_4 to lower-order Li_2S_2 from S_8. The lowest potential plateau is related to the reduction reaction of Li_2S_2 to Li_2S. The third plateau is slightly lower than the second plateau. This may be the main reason why we usually only observe two platforms. Moreover, the increasing $\psi^{o}_{(Li^+/Li)}$ is observed when the dielectric constant value (ε) of the electrolyte goes up, which may be one of the reasons that make differences between the calculations and experimental results. This study should be helpful to raise the potential of the plateau by means of selecting the electrolyte of low dielectric constant value, appropriate smaller concentration of lithium ion and suitable additive. In conclusion, the DFT calculation results would be helpful to better understand the discharge process of sulfur electrode and develop more advanced lithium-sulfur batteries.

References

[1] Ji L W, Rao M M, Zheng H M, Zhang L, Li Y C, Duan W H, Guo J H, Cairns E J, Zhang Y G. *J Am Chem Soc*, 2011, 133: 18522

[2] Chen J, Cheng F Y. *Acc Chem Res*, 2009, 42: 713

[3] Ji X L, Lee K T, Nazar L F. *Nat Mater*, 2009, 8: 500

[4] Ellis B L, Lee K T, Nazar L F. *Chem Mater*, 2010, 22: 691

[5] Jayaprakash N, Shen J, Moganty S S, Corona A, Archer L A. *Angew Chem Int Ed*, 2011, 50: 5904

[6] Yamin H, Gorenshtein A, Penciner J, Sternberg Y, Peled E. *J Electrochem Soc*, 1988, 135: 1045

[7] Kumaresan K, Mikhaylik Y, White R E. *J Electrochem Soc*, 2008, 155: A576

[8] Scrosati B, Hassoun J, Sun Y K. *Energy Environ Sci*, 2011, 4: 3287

[9] Bruce P G, Freunberger S A, Hardwick L J, Tarascon J M. *Nat Mater*, 2012, 11: 19

[10] Barchasz C, Molton F, Duboc C, Leprêtre J C, Patoux S, Alloin F. *Anal Chem*, 2012, 84: 3973

[11] Fu Y Z, Manthiram A. *J Phys Chem C*, 2012, 116: 8910

[12] He G, Ji X L, Nazar L. *Energy Environ Sci*, 2011, 4: 2878

[13] Yang Y, Yu G H, Cha J J, Wu H, Vosgueritchian M, Yao Y, Bao Z N, Cui Y. *ACS Nano*, 2011, 11: 9187

[14] Ji L W, Rao M M, Aloni S, Wang L, Cairns E J, Zhang Y G. *Energy Environ Sci*, 2011, 4: 5053

[15] Bichat M P, Gillot F, Monconduit L, Favier F, Morcrette M, Lemoigno F, Doublet M L. *Chem Mater*, 2004, 16: 1002

[16] Maxisch T, Zhou F, Ceder G. *Phys Rev B*, 2006, 73: 104301

[17] Van der Ven A, Thomas J C, Xu Q C, Swoboda B, Morgan D. *Phys Rev B*, 2008, 78: 104306

[18] Peng B, Cheng F Y, Tao Z L, Chen J. *J Chem Phys*, 2010, 133: 034701

[19] Frisch M J, Trucks G W, Schlegel H B, Frisch M J, Trucks G W et al., GAUSSIAN03, Revision C02, Gaussian, Inc, Pittsburgh, PA 2004

[20] Li L L, Peng B, Ji W Q, Chen J. *J Phys Chem C*, 2009, 113: 3007

[21] Peng B, Li L L, Ji W Q, Cheng F Y, Chen J. *J Alloy Compd*, 2009, 484: 308

[22] Tomasi J, Mennucci B, Cammi R. *Chem Rev*, 2005, 105: 2999

[23] Yang X, Wang G C, Shang Z F, Pan Y M, Cai Z S, Zhao X Z. *Phys Chem Chem Phys*, 2002, 4: 2546

[24] Bogatko S, Geerlings P. *Phys Chem Chem Phys*, 2012, 14: 8058

[25] Meyer B. *Chem Rev*, 1976, 76: 367

[26] Gao J, Lowe M A, Kiya Y, Abruña H D. *J Phys Chem C*, 2011, 115: 25132

[27] Zhang S S. *Electrochim Acta*, 2012, 70: 344

[28] Elazari R, Salitra G, Garsuch A, Panchenko A, Aurbach D. *Adv Mater*, 2011, 23: 5641

[29] He X M, Ren J G, Wang L, Pu W H, Jiang C Y, Wan C R. *J Power Sources*, 2009, 190: 154